

UAV/HAP-Assisted Vehicular Edge Computing in 6G: Where and What to Offload?

Alessandro Traspadini, Marco Giordani, Michele Zorzi

Department of Information Engineering, University of Padova, Italy. Email: {name.surname}@dei.unipd.it

Abstract—In the context of 6th generation (6G) networks, vehicular edge computing (VEC) is emerging as a promising solution to let battery-powered ground vehicles with limited computing and storage resources offload processing tasks to more powerful devices. Given the dynamic vehicular environment, VEC systems need to be as flexible, intelligent, and adaptive as possible. To this aim, in this paper we study the opportunity to realize VEC via non-terrestrial networks (NTNs), where ground vehicles offload resource-hungry tasks to Unmanned Aerial Vehicles (UAVs), High Altitude Platforms (HAPs), or a combination of the two. We define an optimization problem in which tasks are modeled as a Poisson arrival process, and apply queuing theory to find the optimal offloading factor in the system. Numerical results show that aerial-assisted VEC is feasible even in dense networks, provided that high-capacity HAP/UAV platforms are available.

Index Terms—6G, non-terrestrial networks (NTNs), UAV, HAP, offloading, vehicular edge computing (VEC), optimization.

I. INTRODUCTION

Non-terrestrial networks (NTNs) are expected to be a key component of 6th generation (6G) networks, as a means to provide cost-effective and high-capacity connectivity via Unmanned Aerial Vehicles (UAVs), High Altitude Platforms (HAPs), and satellites [1]. For example, NTNs can promote on-demand service continuity when terrestrial towers are out of service (e.g., in emergency situations), and complement terrestrial networks in remote areas, hence representing a promising technology in combating the digital divide [2].

Recently, NTNs have been envisioned to provide 3D flexible coverage and enhanced road safety in Vehicle-to-Everything (V2X) networks [3]. In this context, the success of these networks relies on the availability of massive data from on-board sensors, to guarantee accurate perception of the environment [4]. However, data processing based on machine learning (from compression [5] to object detection and recognition [6], from tracking and trajectory prediction to data dissemination [7]) requires extensive computational resources, which may be challenging for current vehicular terminals [8].

To solve this issue, the research community is investigating vehicular edge computing (VEC), aiming at offloading resource-hungry computation, caching, and/or storage tasks to more powerful edge/distributed servers [9]. While implementing VEC on terrestrial roadside infrastructures may be costly and inefficient [10], aerial-assisted VEC is seen as a valuable solution to satisfy 6G V2X requirements. Equipped with a computing server, UAVs can support ubiquitous broadband connectivity in favorable Line of Sight (LOS) conditions, and the physical proximity between the computing aerial node and

the ground can promote low latency, reliable privacy protection, and high-resolution context awareness. For example the authors in [11] investigated a UAV-enabled offloading system, where the positions of UAVs were optimized to minimize resource consumption, while Hayat *et al.*, in [12], studied edge computing for drone navigation. Lakew *et al.*, in [13], explored the opportunity of data offloading via HAPs, in light of their payload capability, stable deployment in the stratosphere, and large coverage footprint. The potential of HAP-enabled edge computing has been also demonstrated in areas without ground network coverage like countrysides and mountains [14]. The availability of multi-layered hierarchical networks [15], i.e., the orchestration among UAV and HAP platforms, could further enhance VEC performance, and offer higher resilience and flexibility compared to standalone deployments. However, the limited communication range and the inherent latency associated with aerial networks may jeopardize VEC offloading, thereby making the design of these systems not trivial.

Along these lines, in this paper we validate the VEC paradigm for 6G networks, thus we investigate a V2X scenario in which ground vehicles (GVs) offload intensive computing tasks to aerial nodes with rich availability of resources. To do so, we formalize an optimization problem to minimize the processing time under latency and computational capacity constraints. The VEC system is characterized as a set of queues in which tasks are modeled according to a Poisson arrival process, at a rate proportional to the number of GV. Compared to literature papers, we analyze both UAV and HAP layers, and a combination of the two, as a function of several V2X-specific parameters, including the density of GV and the size of the transmitted data. For the first time, we shed light on the optimal computing capacity of GV/UAV/HAPs that guarantees that processing operations never exceed the inter-frame time of the sensors as a means to support real-time V2X services. We demonstrate that there exists an optimal offloading factor resulting in low computational burden on board of vehicles and communication demands. Specifically, HAP-assisted VEC is more desirable than UAV-assisted VEC, which is limited by hardware and energy constraints.

The rest of the paper is organized as follows. In Sec. II we introduce our system model, in Sec. III we present our offloading algorithms, in Sec. IV we discuss our results, whereas conclusions are summarized in Sec. V.

II. SYSTEM MODEL

In this section we present our research problem (Sec. II-A), as well as the delay (Sec. II-B), channel (Sec. II-C) and

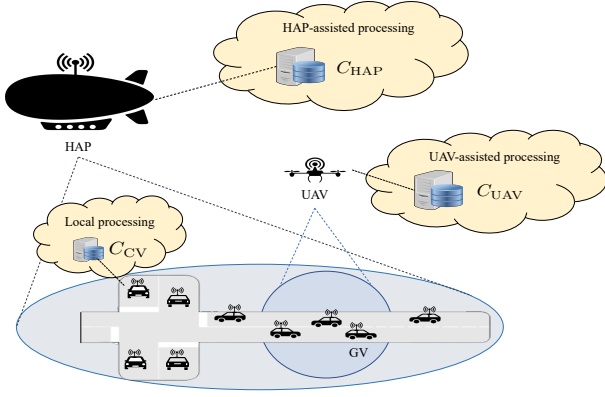


Fig. 1: System model for NTN-assisted VEC.

queuing (Sec. II-D) models.

A. Problem Formulation

We consider a V2X scenario at a road intersection in which k GV/km² are deployed over an Area of Interest (AoI) of A km². The system may be overseen by HAP and/or UAV platforms flying over the AoI; we assume that A is smaller than the coverage footprint shaped by both UAVs and HAPs, as illustrated in Fig. 1.

We analyze the problem of *cooperative perception* where each GV processes sensor's perceptions of n_{UL} bits, generated at a constant rate r , to identify road objects and make intersection crossing decisions accordingly [16]. Each perception involves a constant computational load C for detecting and tracking entities at the intersection [6]. We assume that a fraction $(1 - \eta)C$ of the computational load is processed on board of the GV (local processing), while the remaining computational load ηC is offloaded to NTN servers with high computation and storage capacity (VEC-assisted processing). The optimal offloading factor $\eta^* \in [0, 1]$ must be dimensioned so as to minimize the total processing time.

In the first case, data processing is performed by the GV, offering a limited computation capacity C_{GV} due to the high price of powerful Central Processing Units (CPUs) on board of current low-budget car models. In the second case, data processing is executed at the HAP/UAV's side. While resulting in low computational burden on board, transferring information over a wireless link and processing data at a remote device introduces a non-negligible delay. Despite size, weight, and power limitations, high-end UAVs can be equipped with high-performance computing facilities, and leverage stronger computation capacity than available on board, i.e., $C_{UAV} \geq C_{GV}$ [10]. In addition, HAPs can be operated by solar panels which provide efficient and continuous energy resources, and their large payload permits the installation of high-performance platforms like Graphics Processing Unit (GPU) and Tensor Processing Unit (TPU), to further speed up the computing tasks. As such, the computation capacity of HAPs is $C_{HAP} \geq C_{UAV} \geq C_{GV}$.

B. Delay Model

In this section we evaluate the processing time in case of local or VEC-assisted processing.

a) *Local processing*: The processing time does not involve data offloading to edge servers, and is simply given by:

$$t_{LP}(\eta) = [(1 - \eta)C] / C_{GV}. \quad (1)$$

b) *VEC-assisted processing*: Data offloading requires the wireless transfer of a sensor's perception of size n_{UL} produced on board to NTN servers, and the processed output of size $n_{DL} \leq n_{UL}$ to be sent back to the GV, which results into a capture-to-output delay given by:

$$t_{VEC}(\eta) = 2\tau_p + t_{UL} + t_{DL} + t_{p,VEC}(\eta), \quad (2)$$

where τ_p is the propagation delay, t_{UL} and t_{DL} are the transmissions delays in uplink (UL) and downlink (DL) from the GV to the NTN servers and vice versa, respectively, and $t_{p,VEC}$ is the processing time at the NTN servers, which is studied in Sec. II-D by analyzing the queuing model.

In Eq. (2), τ_p depends on the distance d between the generic GV and the NTN device. Assuming, without loss of generality, that GVs are uniformly distributed over the AoI A , and that the NTN device is placed right above the center of A at an altitude h_0 , we can write the average distance \bar{d} as

$$\bar{d} = \sqrt{\frac{A}{2\pi} + h_0^2}. \quad (3)$$

Thus, the average propagation delay is $\tau_p = \bar{d}/c_0$, where c_0 is the speed of light. The transmission delays, instead, are a function of the capacity of the UL (R_{UL}) and DL (R_{DL}) channels, and the number of vehicles in the system, i.e.,

$$t_\ell = (k \cdot A \cdot n_\ell) / R_\ell, \quad \ell \in \{UL, DL\}. \quad (4)$$

C. Channel Model

VEC involves offloading data to/from edge servers for processing. According to the 3GPP specifications [17], high-capacity transmissions can be established if NTN platforms operate at millimeter waves (mmWaves), where the huge bandwidths available may offer the opportunity of ultra-fast connections via highly directional antennas [18]. According to the 3GPP, the Signal to Noise Ratio (SNR) between transmitter i and receiver j can be computed as

$$\gamma_{ij} = \text{EIRP}_i + (G_j/T) - \text{PL}_{ij} - k - B, \quad (5)$$

where the EIRP is the effective isotropic radiated power, G_j/T is the receive antenna-gain-to-noise-temperature, PL is the path loss, k is the Boltzmann constant, and B is the bandwidth. The EIRP depends on the transmit antenna gain (P_T) and power (G_T) and the cable loss (L_C), and is given by [17]

$$\text{EIRP}_i = P_{T_i} - L_C + G_{T_i}. \quad (6)$$

In turn, the antenna-gain-to-noise-temperature depends on the characteristics of the receiver, and can be computed as

$$\frac{G_j}{T} = G_{R_j} - N_{f_j} - 10 \log_{10} \left[T_{0_j} + (T_{a_j} - T_{0_j}) \cdot 10^{\frac{-N_{f_j}}{10}} \right] \quad (7)$$

where G_R is the receive antenna gain, N_f is the noise figure, and T_0 and T_a are the ambient and antenna temperature.

For the altitude range at which UAVs typically fly (below 500 m), the channel does not involve complete penetration through the atmosphere. Therefore, a simple free-space path loss (FSPL) model can be considered, and we have that

$$\text{PL} = \text{FSPL} = 92.45 + 20 \log_{10}(f_c) + 20 \log_{10}(\bar{d}), \quad (8)$$

where f_c is the carrier frequency expressed in GHz, and \bar{d} is the average distance between the transmitter and the receiver expressed in km. For the HAP channel, instead, the signal in the mmWave bands undergoes several stages of attenuation through the atmosphere, in particular scintillation loss (PL_s , due to sudden changes in the refractive index caused by variation of the temperature, water vapor content, and barometric pressure) and atmospheric absorption loss (PL_g , due to dry air and water vapor attenuation). Hence, the total path loss for HAPs can be expressed as

$$\text{PL} = \text{FSPL} + \text{PL}_g + \text{PL}_s. \quad (9)$$

For a more complete description of the channel model in NTN scenarios, we refer the interested reader to [15].

Based on the channel model described above, we have that the average ergodic (Shannon) capacity R_ℓ shown in Eq. (4), i.e., the maximum achievable data rate, is given by:

$$R_\ell = B \log_2(1 + 10^{\frac{\gamma_{ij}}{10}}), \quad \ell \in \{\text{UL}, \text{DL}\}. \quad (10)$$

D. Queuing Model

Data offloading involves a deterministic amount of time to be resolved, equal to the ratio between the fraction ηC of the computation load that is processed by the NTN node and its computation capacity. This system can be modeled as an M/D/c queue, in which arrivals of offloaded tasks are distributed as a Poisson process, and they are served following a first-come-first-served (FCFS) discipline. The number of servers c is equal to the number of parallel processes that NTN devices can handle, and there is only one waiting line (i.e., single channel queue).

Based on the approximation introduced in [19], the average waiting time in an M/D/c queue is given by

$$W_q(\text{M/D}/c) \approx \frac{1}{2} W_q(\text{M/M}/c), \quad (11)$$

where $W_q(\text{M/M}/c)$ denotes the waiting queuing time for an M/M/c queue, which can be derived from the average length of the M/M/c queue, $L_q(\text{M/M}/c)$, using Little's Law [20], i.e.,

$$W_q(\text{M/M}/c) = L_q(\text{M/M}/c) / \lambda, \quad (12)$$

where $\lambda = r \cdot k \cdot A$ is the arrival rate. $L_q(\text{M/M}/c)$ is computed as

$$L_q(\text{M/M}/c) = \frac{G}{c - G} \cdot \mathcal{C}(c, G), \quad (13)$$

where G is the offered traffic, i.e., the ratio between the arrival rate and the service rate (that is $\mu = C_i / (\eta C)$, for

$i \in \{\text{UAV}, \text{HAP}\}$), and $\mathcal{C}(c, G)$ is the probability that all the servers are busy and it is obtained as

$$\mathcal{C}(c, G) = \frac{1}{\sum_{r=0}^{c-1} \frac{G^r}{r!} + \frac{c \cdot G^c}{c!(c-G)}} \cdot \frac{c \cdot G^c}{c!(c-G)}. \quad (14)$$

From the waiting time in Eq. (11), we have that the processing time for offloading at the VEC servers shown in Eq. (2) can be computed, for $i \in \{\text{UAV}, \text{HAP}\}$, as

$$t_{p, \text{VEC}}(\eta) = W_q(\text{M/D}/c) + (1/\mu) = W_q(\text{M/D}/c) + \frac{\eta C}{C_i}. \quad (15)$$

III. OPTIMAL OFFLOADING FOR NTN-ASSISTED VEC

In this section we formalize an optimization problem to identify the optimal offloading factor η^* to minimize the total processing time. In case of VEC-assisted processing, we distinguish between standalone (Sec. III-A) and hybrid (Sec. III-B) offloading, depending on whether or not UAVs' and HAPs' computing facilities are used in combination.

A. Standalone Offloading

In this case, a fraction η_i^* , $i \in \{\text{UAV}, \text{HAP}\}$, of the computational load C is offloaded to either UAV or HAP platforms, that operate individually. The optimization problem in this configuration can be written as:

$$\begin{aligned} \arg \min_{\eta_i} \quad & \max [t_{\text{LP}}(\eta_i), t_{\text{VEC}}(\eta_i)], \\ \text{subject to} \quad & G(\eta_i) < c, \end{aligned} \quad (16a)$$

$$\eta_i \in [0, 1]. \quad (16b)$$

Constraint (16a) is necessary to keep the queue stable, which gives the following upper bound for η_i , i.e.,

$$G(\eta_i) < c \Rightarrow \eta_{i, \max} = \frac{c \cdot C_i}{C \cdot k \cdot A \cdot r}. \quad (17)$$

The problem can be solved following an iterative procedure. If $t_{\text{LP}}(\eta_i) < t_{\text{VEC}}(\eta_i)$, data offloading is not convenient compared to local processing, and eventually results in an additional overhead due to data transmission to/from NTN platforms. In this condition, the optimal solution would be to set $\eta_i^* = 0$ (fully-local processing). Otherwise, it can be shown that the optimal solution of the problem is

$$t_{\text{LP}}(\eta_i^*) = t_{\text{VEC}}(\eta_i^*). \quad (18)$$

For simplicity, the algorithm stops when the difference between t_{LP} and t_{VEC} satisfies the following condition:

$$|t_{\text{LP}}(\ell) - t_{\text{VEC}}(\ell)| < \xi \cdot t_{\text{VEC}}(\ell). \quad (19)$$

The correctness of the algorithm is given by the fact that t_{LP} and t_{VEC} are, respectively, monotonically increasing and monotonically decreasing functions.

B. Hybrid Offloading

Initial studies have demonstrated that the availability of multi-layered hierarchical networks represents a promising technology to solve coverage and latency constraints in NTN scenarios [15]. Therefore we analyzed the case in which GVs

TABLE I: System parameters.

Parameter	GV	UAV	HAP
Sensor's perception rate (r) [fps]		10	
Sensor's perception size (n_{UL}) [Mb]		1	
Processed data size (n_{DL}) [Mb]		0.1	
Computational load (C) [GFLOP]		100	
Density of GVs (k) [GV/km ²]		[25,500]	
Area of interest (A) [km ²]		1	
Carrier frequency (f_c) [GHz]		38	
Bandwidth (B) [MHz]		400	
Altitude (h_0) [km]	0	0.1	20
Path loss (PL) [dB]	N/A	101.98	172.76
EIRP [dBW]	29	-10	27.9
Rx. gain/noise temperature (G/T) [dB/K]	12.15	-11.6	27.7
Computational capacity (C_i) [GFLOP/s]	500	1500	3500
Maximum number of servers (c_i)	1	4	12

can offload data to both UAV and HAP simultaneously. The optimization problem is described as follows:

$$\begin{aligned} \arg \min_{\eta_{UAV}, \eta_{HAP}} \quad & \max [t_{VEC}(\eta_{UAV}), t_{VEC}(\eta_{HAP}), t_{LP}(\eta_{UAV} + \eta_{HAP})], \\ \text{subject to} \quad & G(\eta_{UAV}) < c_{UAV}, G(\eta_{HAP}) < c_{HAP}, \\ & \eta_{HAP}, \eta_{UAV}, \eta_{HAP} + \eta_{UAV} \in [0, 1]. \end{aligned} \quad (20a)$$

$$(20b)$$

Constraints (20a) are derived from Eq. (17), and are necessary to keep both UAV and HAP queues stable, where $G(\eta_{UAV})$ and $G(\eta_{HAP})$ are the offered traffic, and c_{UAV} and c_{HAP} are the number of servers of UAVs or HAPs, respectively.

The problem can be solved following a two-step procedure.

- *Step 1:* Identify the optimal offloading factor η_{UAV}^* for the computational load C in case of standalone UAV offloading. This problem is solved through the procedure described in Sec. III-A for standalone UAV offloading, which requires a total processing time $t_{SO,UAV}^*$.
- *Step 2:* Evaluate whether HAPs can reduce the total processing time $t_{SO,UAV}^*$. If $t_{SO,UAV}^* < t_{VEC}(\eta_{HAP})$, HAP-assisted offloading is not convenient compared to standalone UAV offloading. In this condition, the optimal solution would be to set $\eta_{HAP}^* = 0$. Otherwise, hybrid offloading is desirable, and it can be shown that the optimal solution of the problem is

$$t_{VEC}(\eta_{HAP}^*) = t_{SO,UAV}^*. \quad (21)$$

For simplicity, the algorithm stops when we have:

$$|t_{VEC}(\eta_{HAP}^*) - t_{SO,UAV}^*| < \xi \cdot t_{VEC}(\eta_{HAP}^*) \quad (22)$$

IV. PERFORMANCE EVALUATION

In this section, after introducing our simulation setup, we evaluate the performance of the proposed offloading schemes in different V2X scenarios.

A. Simulation Setup and Parameters

Simulation parameters, if not otherwise specified, are reported in Table I. Our scenario consists of an area of size $A = 1$ km², where k GV/km² are deployed according to a Poission Point Process (PPP). All devices operate at $f_c = 38$ GHz, with a bandwidth of $B = 400$ MHz.

Each GV produces a sensor's perception (e.g., an RGB camera image) of size $n_{UL} = 1$ Mb, at a constant rate $r = 10$ fps. Each perception involves a constant computational load $C = 100$ GFLOP for V2X-related processing (e.g., object detection and classification), and the processed output (e.g., bounding boxes) is eventually returned to the GVs in a packet of size $n_{DL} = 0.1$ Mb. GVs, UAVs and HAPs have a computational capacity of $C_{GV} = 500$, $C_{UAV} = 1500$ and $C_{HAP} = 3000$ GFLOP/s, respectively. However, as the performance of computing hardware continues to hit new milestones, it is expected that connected/automated cars, as well as UAV/HAP platforms, will have more computing power in the future. To capture this, numerical results will be given considering a range of values for the computational capacity, to simulate different computing conditions.

The performance of the offloading schemes in Sec. III are evaluated in terms of the total time it takes to process the computational load C , as a function of the density of GVs, the size of the transmitted data, as well as the processing capability of the nodes. Ideally, the processing time should be lower than the frame rate r of the sensors (100 ms in our scenario), so as to ensure real-time driving responses.

B. Numerical Results

1) *Users density:* In Figs. 2 and 3 we evaluate the minimum processing time (and relative optimal offloading factor) for different offloading schemes, as a function of the density of GVs k and the on-board computational capacity C_{GV} . In Fig. 2 each group of bar plots represents, respectively, standalone UAV offloading (SO UAV), standalone HAP offloading (SO HAP), and hybrid offloading (HO), respectively. We can see that, when $k = 25$ (200), the optimal offloading factor for SO UAV is as low as 20% (5%), regardless of C_{GV} . This is due to the scarce computational capacity available to UAVs: despite the favorable channel, by offloading more tasks, the UAV queue would become unstable, i.e., $G(\eta_{UAV}) > c_{UAV}$. For $C_{GV} = 200$ GFLOP/s (Fig. 3a), the total processing time for SO UAV is similar to that of fully-local computation, and is above 400 ms even in sparsely deployed networks, which is incompatible with the requirements of most 5G/6G V2X applications. For $C_{GV} = 1000$ GFLOP/s (Fig. 3b), the processing time becomes lower than 100 ms, i.e., the frame rate of the sensors, which however involves higher hardware costs and energy consumption on board.

In turn, SO HAP has access to more powerful computational resources and, despite the severe path loss, can support up to 95% (70%) of the computational load when $C_{GV} = 200$ (1000) GFLOP/s, for $k = 25$. In this configuration the processing time is lower than 100 ms when $k < 50$ even for $C_{GV} = 200$ GFLOP/s. Notice that more populated scenarios (e.g., $k > 200$) may overload the available channel bandwidth, and result in very long transmission delays: in this case fully-local processing is the most desirable option.

As expected, the best scenario is the HO scheme, in which UAV and HAP nodes cooperate together to reduce the processing time. Nevertheless, the performance is similar to that of

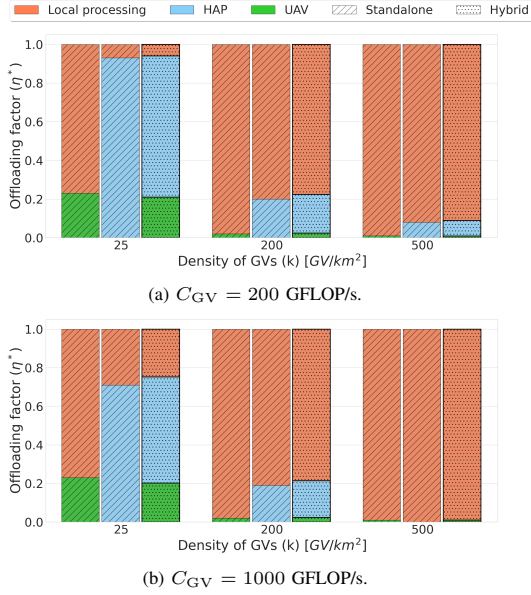


Fig. 2: Total processing time for different offloading schemes, vs. C_{GV} and k .

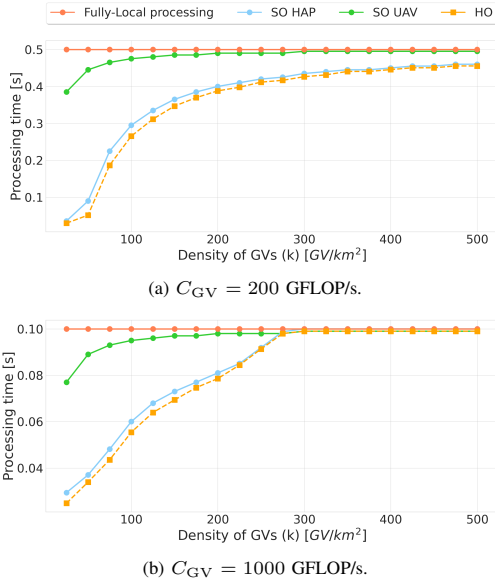


Fig. 3: Offloading factor for different offloading schemes, vs. C_{GV} and k .

the SO HAP scheme, while in turn resulting in more complex and expensive network management.

2) *Sensor's perception size*: In this second set of simulations we evaluate the impact of the sensor's perception size n_{UL} , which affects the transmission time for offloading described in Eq. (4) and, thus, the total processing time.

In Fig. 4a we recognize two regimes for both the SO HAP and HO configurations when $k = 200$. When $n_{UL} < 2.5$ Mb, the total processing time is constant with n_{UL} . In this region, at most 20% of the computational load can be offloaded to the HAP platform to maintain the system stable (Fig. 2), which means that the remaining 80% of the computational tasks have to be processed on board: this requires around

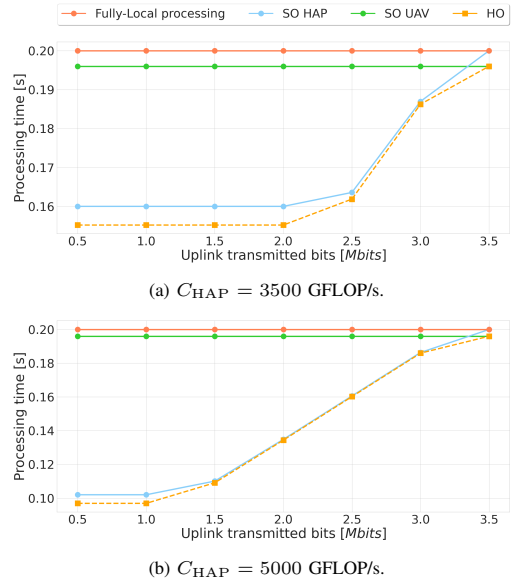


Fig. 4: Total processing time for different offloading schemes and $k = 200$, vs. C_{HAP} and n_{UL} .

160 ms, regardless of the size of the perception data. When $n_{UL} > 2.5$ Mb, instead, the total processing time grows linearly with n_{UL} . In this region the transmission time for offloading becomes so large that it exceeds the time for local processing, which then becomes more desirable. On the other hand, in the SO UAV configuration, the impact of n_{UL} is negligible: the very low path loss experienced in the UAV channel results in a very low transmission delay, regardless of the size of the data. The bottleneck is given by the UAV queue: given that less than 5% of the computational load can be offloaded to the UAV platform (Fig. 2), the processing time is similar to the case of local processing, and is around 200 ms.

From Fig. 4a it appears clear that, even in the most convenient architecture, the total processing time is always above 100 ms (our target requirement for real-time operations). Better results can be obtained by considering more powerful offloading platforms. For example, in Fig. 4b we see that, with a HAP with $c_{HAP} = 20$ servers, each of which has a computational capacity of $C_{HAP} = 5000$ GFLOP/s, the total processing time is maintained below the threshold of 100 ms as long as $n_{UL} < 1.2$ Mb.

3) *UAV/HAP computational capacity*: As discussed above, the performance of the system is constrained by the capacity of the queues at the NTN servers, which can be expanded by increasing the computing power. This is validated in Fig. 5 considering a scenario with $k = 200$ GV/km², where we plot the processing time as a function of the computational capacity of UAVs and HAPs. For UAVs, C_{UAV} ranges between 1000 and 4000 GFLOP/s, whereas c_{UAV} varies between 2 and 8. For HAPs, C_{HAP} ranges between 3000 and 10000 GFLOP/s, whereas c_{HAP} varies between 6 and 25.

From Fig. 5 (up) we can see that, as the UAV becomes more powerful, the probability of offloading grows accordingly, which has the benefit to decrease the total processing time by up to 70% compared to the baseline SO UAV results in Fig. 3a.

ACKNOWLEDGMENTS

Part of this work was supported by the US Army Research Office under Grant no. W911NF1910232.

REFERENCES

- [1] M. Giordani and M. Zorzi, "Non-Terrestrial Networks in the 6G Era: Challenges and Opportunities," *IEEE Network*, vol. 35, no. 2, pp. 244–251, Dec. 2021.
- [2] A. Chaoub, M. Giordani, B. Lall, V. Bhatia, A. Kliks, L. Mendes, K. Rabie, H. Saarnisaari, A. Singhal, N. Zhang, S. Dixit, and M. Zorzi, "6G for Bridging the Digital Divide: Wireless Connectivity to Remote Areas," *IEEE Wireless Communications*, July 2021.
- [3] S. S. Shinde and D. Tarchi, "Towards a Novel Air–Ground Intelligent Platform for Vehicular Networks: Technologies, Scenarios, and Challenges," *Smart Cities*, vol. 4, no. 4, pp. 1469–1495, Dec. 2021.
- [4] S. Zhang, J. Chen, F. Lyu, N. Cheng, W. Shi, and X. Shen, "Vehicular communication networks in the automated driving era," *IEEE Communications Magazine*, vol. 56, no. 9, pp. 26–32, Sep. 2018.
- [5] F. Nardo, D. Peressoni, P. Testolina, M. Giordani, and A. Zanella, "Point Cloud Compression for Autonomous Driving: A Performance Comparison," in *IEEE Wireless Communications and Networking Conference (WCNC) [To Appear]*, 2022.
- [6] V. Rossi, P. Testolina, M. Giordani, and M. Zorzi, "On the Role of Sensor Fusion for Object Detection in Future Vehicular Networks," in *Joint European Conference on Networks and Communications 6G Summit (EuCNC/6G Summit)*, 2021.
- [7] M. Baek, D. Jeong, D. Choi, and S. Lee, "Vehicle trajectory prediction and collision warning via fusion of multisensors and wireless vehicular communications," *Sensors*, vol. 20, no. 1, p. 288, Jan. 2020.
- [8] A. Belogaev, A. Elokhin, A. Krasilov, E. Khorov, and I. F. Akyildiz, "Cost-Effective V2X Task Offloading in MEC-Assisted Intelligent Transportation Systems," *IEEE Access*, vol. 8, Sept. 2020.
- [9] L. Liu, C. Chen, Q. Pei, S. Maharjan, and Y. Zhang, "Vehicular edge computing and networking: A survey," *Mobile networks and applications*, vol. 26, no. 3, pp. 1145–1168, Jun 2021.
- [10] J. Hu, C. Chen, L. Cai, M. R. Khosravi, Q. Pei, and S. Wan, "UAV-Assisted Vehicular Edge Computing for the 6G Internet of Vehicles: Architecture, Intelligence, and Challenges," *IEEE Communications Standards Magazine*, vol. 5, no. 2, pp. 12–18, June 2021.
- [11] S. Sun, G. Zhang, H. Mei, K. Wang, and K. Yang, "Optimizing Multi-UAV Deployment in 3-D Space to Minimize Task Completion Time in UAV-Enabled Mobile Edge Computing Systems," *IEEE Communications Letters*, vol. 25, no. 2, pp. 579–583, Oct. 2021.
- [12] S. Hayat, R. Jung, H. Hellwagner, C. Bettstetter, D. Emini, and D. Schnieders, "Edge computing in 5G for drone navigation: What to offload?" *IEEE Robotics and Automation Letters*, vol. 6, no. 2, pp. 2571–2578, Apr. 2021.
- [13] D. S. Lakew, A.-T. Tran, N.-N. Dao, and S. Cho, "Intelligent Offloading and Resource Allocation in HAP-Assisted MEC Networks," in *International Conference on Information and Communication Technology Convergence (ICTC)*, 2021.
- [14] M. Ke, Z. Gao, Y. Huang, G. Ding, D. W. K. Ng, Q. Wu, and J. Zhang, "An Edge Computing Paradigm for Massive IoT Connectivity over High-Altitude Platform Networks," *IEEE Wireless Communications*, vol. 28, no. 5, pp. 102–109, Jun. 2021.
- [15] D. Wang, M. Giordani, M.-S. Alouini, and M. Zorzi, "The Potential of Multi-Layered Hierarchical Non-Terrestrial Networks for 6G: A Comparative Analysis Among Networking Architectures," *IEEE Vehicular Technology Magazine*, vol. 16, no. 3, pp. 99–107, Sep. 2021.
- [16] T. Higuchi, M. Giordani, A. Zanella, M. Zorzi, and O. Altintas, "Value-anticipating V2V communications for cooperative perception," in *IEEE Intelligent Vehicles Symposium (IV)*, 2019.
- [17] 3GPP, "Solutions for NR to support Non-Terrestrial Networks (NTN)," TR 38.821 (Release 16), 2020.
- [18] M. Giordani and M. Zorzi, "Satellite Communication at Millimeter Waves: a Key Enabler of the 6G Era," *IEEE International Conference on Computing, Networking and Communications (ICNC)*, Feb 2020.
- [19] W. Whitt, "Queueing network analyzer." *The Bell System Technical Journal*, vol. 62, pp. 2779–2815, 11 1983.
- [20] N. Benvenuto and M. Zorzi, *Principles of Communications Networks and Systems*. Wiley, 2011.

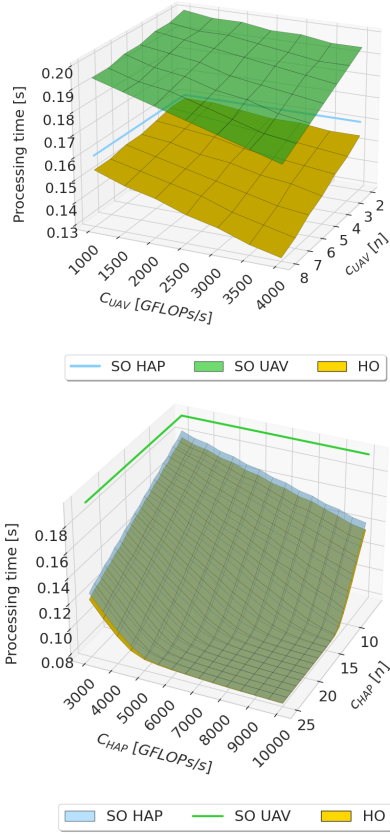


Fig. 5: Total processing time for different offloading schemes, vs. the UAV (up) and HAP (down) computational capacity, for $k = 200$.

However, even considering HO, the processing time is still above the threshold of 100 ms, an indication that increasing the UAV's capacity alone is not enough to support V2X operations at the frame rate of the sensors. To achieve this objective, it is necessary to increase C_{HAP} , as illustrated in Fig. 5 (down): in this case, the processing time is below 100 ms as long as $C_{HAP} > 5000$ GFLOP/s and $C_{HAP} > 15$.

V. CONCLUSIONS AND FUTURE WORKS

In this paper we shed light on the potential of NTN-assisted VEC for 6G systems. To do so, we considered a V2X scenario at a road intersection in which vehicles can decide to either process data on board, or offload a fraction of their computational load to UAVs and/or HAPs. Then, we formalized an optimization problem to find the optimal dimensioning of the computational capacity of GVs, UAVs, and HAPs to minimize the total processing time. From our simulations, we demonstrated that HAP-assisted VEC can reduce the processing time compared to fully-local processing, despite the transmission time required for offloading data to/from edge servers. We also showed that hybrid NTN offloading can further improve the processing performance, while incurring non-negligible hardware and computing costs.

As part of our future work we will consider end-to-end system-level simulations. Moreover, we will extend our optimization problem to incorporate the impact of the energy consumption on the offloading performance.